Published in final edited form as:

Anal Chem. 2022 March 15; 94(10): 4236–4242. doi:10.1021/acs.analchem.1c04485.

Two-Dimensional Fractionation Method for Proteome-Wide Cross-Linking Mass Spectrometry Analysis

Fenglong Jiao[1], **Clinton Yu**[1], **Andrew Wheat**[1], **Xiaorong Wang**[1], **Scott D. Rychnovsky**[2], **Lan Huang**[1,*]

[1]Department of Physiology & Biophysics, University of California, Irvine, Irvine, CA 92694, USA

[2]Department of Chemistry, University of California, Irvine, Irvine, CA 92694, USA

Abstract

Cross-linking mass spectrometry (XL-MS) is an emergent technology for studying protein-protein interactions (PPIs) and elucidating architectures of protein complexes. The development of various MS-cleavable cross-linkers has facilitated the identification of cross-linked peptides, enabling XL-MS studies at the systems level. However, the scope and depth of cellular networks revealed by current XL-MS technologies remain limited. Due to the inherently broad dynamic range and complexity of proteomes, interference from highly abundant proteins impedes the identification of low abundance cross-linked peptides in complex samples. Thus, peptide enrichment prior to MS analysis is necessary to enhance cross-link identification for proteome-wide studies. Although chromatographic techniques including size exclusion (SEC) and strong cation exchange (SCX) have been successful in isolating cross-linked peptides, new fractionation methods are still needed to further improve the depth of PPI mapping. Here, we present a two-dimensional (2D) separation strategy by integrating peptide SEC with tip-based high pH reverse-phase (HpHt) fractionation to expand the coverage of proteome-wide XL-MS analyses. Combined with the MS-cleavable cross-linker DSSO, we have successfully mapped *in vitro* PPIs from HEK 293 cell lysates with improved identification of cross-linked peptides compared to existing approaches. The method developed here is effective and can be generalized for cross-linking studies of complex samples.

Graphical Abstract

*Correspondence should be addressed to Dr. Lan Huang (lanhuang@uci.edu), Medical Science I, D233, Department of Physiology & Biophysics, University of California, Irvine, Irvine, CA 92697-4560, Phone: (949) 824-8548, Fax: (949) 824-8540.

CONFLICT OF INTEREST

The authors declare no conflict of interest

Supporting Information for Publication

The Supporting Information is available free of charge at https://pubs.acs.org/doi/10.1021/acs.analchem.1c04485.

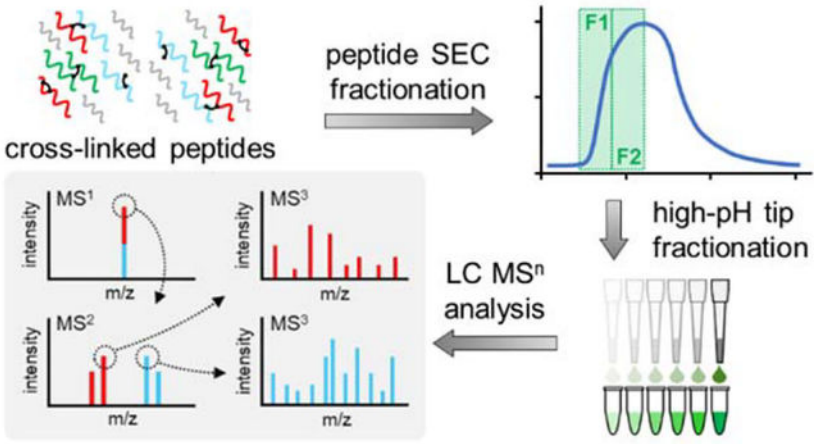

INTRODUCTION

Proteins are functional components in mediating a wide range of biological processes, rarely acting alone in cells. It has been reported that more than 80% of proteins form multi-subunit protein complexes through protein-protein interactions (PPIs) to fulfill their functional roles.[1] Characterization of PPIs contributes to understanding the assembly, structure, function, and dynamics of protein complexes, providing molecular details linking them to cell biology and human pathologies. Affinity purification mass spectrometry (AP-MS) has been particularly successful in proteome-wide PPI studies, and recently yielded a comprehensive human interactome with 118,162 interactions among 14,586 proteins.[2] Despite its effectiveness, AP-MS analysis can only reveal PPI identities—it is incapable of delineating direct and indirect interactions. Furthermore, AP-MS experiments require cell engineering to express tagged baits for affinity purification, which may complicate protein interactions and functions. Therefore, alternative strategies are needed to complement AP-MS based PPI studies. In recent years, cross-linking mass spectrometry (XL-MS) has become an emergent technology for studying PPIs *in vivo* and *in vitro* at the systems-level due to its unique capability of capturing native PPIs from cellular environments.[3–13] Identification of cross-linked peptides allows the determination of PPI identities and contacts simultaneously. In addition, the distances between two cross-linked residues defined by a given cross-linker can function as distance constraints to assist in refining existing structures and elucidating architectures of protein complexes through computational modeling.[14,15] Importantly, proteome-wide XL-MS analysis is suited for high-throughput PPI mapping from various sample origins without the need for cell engineering.

In XL-MS studies, unambiguous identification of cross-linked peptides is critical for determining PPI contacts but inherently challenging—especially for complex samples. Recent developments in cross-linking reagents, bioinformatics tools, and MS instrumentation have facilitated the identification of cross-linked peptides and enabled proteome-wide XL-MS studies.[3–6] Among them, MS-cleavable cross-linker based platforms have played a significant role in advancing global PPI mapping of proteomes from intact cells,[7,10,16] cell lysates,[8,9,13] and tissues.[17] While an *in vivo* XL-proteome composed of

2484 proteins analysis has been recently mapped,[7] further developments are still needed to expand the scope of XL-proteomes to the level of MS proteomes uncovered by shotgun proteomics. Due to the extremely broad dynamic range of proteomes, it remains challenging to detect and identify cross-linked peptides from low-abundance proteins. Therefore, cross-link enrichment is critical for successful proteome-wide XL-MS experiments. Isolation of cross-linked peptides has been accomplished through various strategies including affinity tag[7,16–19] and chromatography-based enrichment methods.[12,20–25] Affinity tags can be directly incorporated in cross-linkers or conjugated through click-chemistry. Chromatographic techniques such as strong cation exchange (SCX), size exclusion (SEC) and hydrophilic interaction liquid chromatography (HILIC) have been employed for XL-MS studies. While successful, these techniques have limited separation resolution, which leads to cross-linked peptides being relatively concentrated in a few fractions. Thus, the complexity of resulting fractionated samples remains high for proteome analysis. To further improve the separation of cross-linked peptides to enhance their MS detection, two-dimensional (2D) separation strategies by integrating orthogonal chromatographic techniques have been developed, e.g., ChaFRADIC[22] and SCX-hSAX.[23] However, a large number of fractions (e.g., 18–30 fractions) are commonly collected and extended chromatographic gradients are needed for LC MS to achieve in-depth analysis, leading to extensive usage of instrument time for proteome-wide XL-MS studies[25]. Therefore, new analytical strategies are still needed to advance XL-MS studies of complex samples with improved efficiency and throughput.

In comparison to peptide separation techniques such as SCX that require salt gradients, high pH reverse-phase (HpH) chromatography is advantageous as it uses the same solvents as low pH LC for MS analysis and has proven effective in reducing sample complexity and enhancing the identification of low abundance peptides in complex samples for bottom-up proteomic studies.[26,27] In addition, the salt-free nature eliminates the need for a desalting step prior to LC MS, minimizing sample loss. However, the potential of HpH separation has not been fully explored in XL-MS studies. Here, we present a 2D fractionation method for proteome-wide XL-MS experiments by integrating peptide SEC with tip-based high pH RP (HpHt) fractionation to separate cross-linked peptides prior to MS analysis. In combination with the MS-cleavable cross-linker DSSO, we have identified 10,932 unique cross-linked peptides from human HEK293 cell lysates. This XL-MS data set contained 780 CORUM protein complexes, including the ribosome, pre-RNA spliceosome and 26S proteasome. Our results have demonstrated that the two-dimensional separation strategy developed here is effective and can be directly applicable for other proteome-wide XL-MS studies in the future.

EXPERIMENTAL PROCEDURES

Materials and Reagents

General chemicals for buffers and cell culture media were purchased from Fisher (Waltham, MA) or VWR (Radnor, PA). Sequencing grade trypsin was purchased from Promega (Madison, WI).

DSSO Cross-Linking of HEK 293 Cell Lysates

The HEK 293 cells were cultured in Dulbecco's modified Eagle's medium (DMEM) supplemented with 10% fetal bovine serum (FBS) and 1% penicillin-streptomycin until 90% confluence as previously described.[7] After washing with PBS three times, cell pellets were resuspended in lysing buffer (100 mM sodium chloride, 50 mM sodium phosphate, 10% glycerol, 2 mM ATP, 1 mM TCEP, 10 mM $MgCl_2$, 1x protease inhibiter (Roche), 1× phosphatase inhibitor, and 0.5% NP-40, pH 7.5). The cell debris was removed by centrifugation at 13,000 rpm for 15 min at 4 °C. The supernatant was collected and adjusted to 1 mg/ml, which was subjected to cross-linking with 2 mM DSSO at room temperature for 1 h. The cross-linking reaction was quenched with 50 mM ammonium bicarbonate for 10 min.

SEC-HpHt Fractionation

Cross-linked cell lysates were digested as previously described[7] (Supplemental Methods). Two hundred and fifty micrograms of desalted peptides in 30% ACN/0.1% FA were loaded onto a Superdex™ Peptide 3.2/300 SEC column for separation.[21] The two SEC fractions containing cross-linked peptides were collected, dried, dissolved in 160 μL of ammonia water (pH 10), and subjected to HpHt fractionation separately (Supplemental Methods).

Identification of Cross-Linked Peptides by LC MS^n

Cross-linked peptides were analyzed by LC MS^n using an UltiMate 3000 RSLC (Thermo Fisher, San Jose, CA) coupled to an Orbitrap Fusion Lumos mass spectrometer (Thermo Fisher, San Jose, CA) as described.[28] MS^n data were extracted using MSConvert (ProteoWizard 3.0.10738) and subjected to database searching using Protein Prospector (v.6.3.3). Cross-linked peptides were identified by the integration of MS^n data with database search results using the in-house software xl-Tools[28] (Supplemental Methods).

PPI Analysis and Structural Mapping

XL-PPI networks were generated from the pairwise interactions determined by *in vitro* cross-linking. CORUM (http://mips.helmholtz-muenchen.de/corum), BioPlex (https://bioplex.hms.harvard.edu/), and BioGrid (https://thebiogrid.org/) were used to annotate and determine protein complexes. Functional enrichment was performed using the Gene Ontology Consortium (http://www.geneontology.org). Cross-link mapping to high-resolution structures of protein complexes was performed as described[7] (Supplemental Methods).

RESULTS AND DISCUSSION

Developing a 2D Fractionation Method for Proteome-Wide XL-MS Analysis

To enhance the depth of proteome-wide XL-MS analysis, we aimed to develop a robust analytical workflow that enables improved peptide separation to expand the dynamic range. To this end, we have designed a 2D fractionation method coupling peptide SEC with tip-based HpH separation (SEC-HpHt) and evaluated its efficiency using DSSO cross-linked HEK293 cell lysates. As illustrated in Figure 1, SEC was first performed on a cross-linked digest mixture to separate interlinked peptides from non-cross-linked peptides

and linear cross-linked products (i.e., dead-end and intralinked peptides), yielding 2 SEC fractions. Each SEC fraction was then subjected to HpHt separation to further reduce peptide complexity, resulting in six salt-free, LC MS-ready fractions. Thus, for each XL-MS experiment, a total of 12 SEC-HpHt fractions were generated and analyzed by LC MS^n.[29] Each fraction was analyzed over a 2 h LC gradient, for a total 24 h of MS acquisition time—much faster than published lysate XL-MS analyses[9,12] (Table S1).

Evaluation of SEC-HpHt Separation

To investigate the benefit of incorporating HpHt separation to the SEC-based XL-MS workflow, we compared the number of cross-linked peptides identified from an SEC fraction with and without HpHt separation. Without HpHt separation, the total number of cross-linked peptides identified from the SEC fraction was 818, signifying 741 unique K-K linkages from 375 proteins. When the same SEC sample was further separated into six HpHt fractions for LC MS^n analysis, a total of 6205 cross-linked peptides were identified, representing 4260 unique K-K linkages from 1357 proteins. Our results indicate that the 2D separation considerably increased the identification of both cross-links and cross-linked proteins. With the intensity-based absolute quantification (iBAQ) values of the HEK293 proteome,[30] we plotted the abundance distribution of the identified cross-linked proteins, based on which HpHt separation appeared to significantly improve the dynamic range of XL-MS analysis (Figure S1).

To understand the effectiveness of HpHt separation, we plotted the distribution of cross-linked peptides identified from every SEC-HpHt fraction. As shown, unique cross-linked peptides were identified from each fraction (Figure S2A). On average, 37% and 51% cross-linked peptides identified from each SEC1-HpHt and SEC2-HpHt fraction were unique, respectively. Cumulatively, 67% of all cross-linked peptides were found only in a single fraction, 25% were identified in two fractions, and 5% were identified in three or more fractions altogether, accounting for 97% of all cross-link identifications (Figure S2B). These results indicate that the HpHt fractionation step is highly efficient.

We next examined the orthogonality of the HpHt and LC MS by comparing the retention time of cross-linked peptides in the SEC-HpHt fraction during LC MS^n runs. Since increased concentrations of acetonitrile were used to elute peptides in both HpHt and LC MS separation, we concatenated a total of 10 SEC-HpHt fractions into six fractions in a similar manner to high-low-pH RP shotgun proteomics studies.[26] As shown in Figure 2, cross-linked peptides in each SEC-HpHt fraction eluted evenly across the 2 h LC gradient. Taken together, HpHt fractionation is well-suited for coupling with SEC, and their integration is effective in enhancing the separation and identification of cross-linked peptides during LC MS^n analysis.

Evaluation of the SEC-HpHt Workflow for Proteome-Wide XL-MS Analysis

To assess the performance of the SEC-HpHt workflow for complex XL-MS studies (Figure 1), we have repeated DSSO-based XL-MS experiments of HEK293 cell lysates for a total of three biological replicates—36 LC MS^n acquisitions altogether. The distribution of cross-linked peptides identified across all SEC-HpHt fractions is shown in Figure 3. Based on

43,297 CSMs, 10,932 unique DSSO cross-linked peptides were identified from all samples at 0.3% FDR, representing 8601 unique K-K linkages that describe an XL-proteome of HEK 293 cells lysates composed of 2066 human proteins (Table S2).

To evaluate the breadth of information yielded by the XL-MS workflow established here, we compared our XL-proteome to those of two published DSSO XL-MS data sets of mammalian cell lysates[9,12]. The first data set was generated from HeLa cell lysate in a duplicate experiment, in which cross-linked peptides were separated by off-line SCX into 42 fractions and analyzed by integrated ETD-MS2 and CID-MS3 for a combined 126 h, yielding an XL-proteome composed of 1350 proteins with a total of 3689 cross-linked peptides at 2% FDR.[9] In comparison, our HEK293 XL-proteome is roughly ~1.5-fold larger (2066 vs 1350) and covered ~69% (926/1350) of the Hela XL-proteome (Figure S3). The second DSSO XL-MS data set—generated from cross-linked K562 cell lysate—utilized either SCX or HILIC chromatography separation for a total of 344 LC MS^n acquisitions.[12] This extensive peptide fractionation resulted in the identification of 9319 unique cross-links from 2645 proteins, therefore representing the largest *in vitro* XL-MS data set reported thus far and sharing a 42.8% similarity in identified cross-linked proteins with our XL-proteome. However, when comparing the total utilized MS acquisition time (72 vs >1000 h) to the number of identified cross-linked proteins (2066 vs 2645) and unique cross-links (8601 vs 9319) generated in both data sets, the SEC-HpHt workflow proved to be more efficient as it produced a similar breadth of information with significantly less time (Table S1).

During the course of our study, Zhang et al. have coupled HpH LC with tip-based SCX to improve cross-link identification, which resulted in the identification of 4352 DSSO cross-linked peptides from 2240 proteins in a triplicate experiment.[24] In comparison, our 2D separation workflow identified ~2.5-fold more cross-linked peptides. To determine the robustness of our XL-MS workflow, we examined data reproducibility of our XL-MS experiments with HEK 293 cell lysates. We compared the unique K-K linkages and pair-wise PPIs in our data sets and found 34% and 35% overlaps among the three biological replicates, respectively (Figure 4A, B). These results are comparable to or better than existing proteome-wide XL-MS studies.[7,8] Given the limited overlaps among biological replicates, it is noted that the overall number of cross-links identified in an XL-MS experiment would also be dependent on the number of replicates. Nonetheless, the SEC-HpHt strategy established here has demonstrated its effectiveness and robustness in improving proteome-wide XL-MS analysis.

Validation of Cross-Links by Structural Mapping

In this work, our XL-proteome revealed a total of 780 CORUM protein complexes, among which 75.9% were identified with ≥ 50% protein composition (Figure 4C and Table S3). To assess cross-link validity, we mapped a total of 1330 K-K linkages onto the available high-resolution structures of 111 protein complexes (Table S4A). As a result, 83% of cross-links have a Cα-Cα distance within the maximum distance confined by DSSO (≤ 30 Å), with an overall distribution centering around 16.6 Å (Figure 5A and Table S4A), supporting the reliability of the identified cross-links.

Among the protein complexes identified, the 26S proteasome was well represented with 75 K-K linkages, describing 25 PPIs among 23 out of 33 subunits. When mapped to the high-resolution structure of the human 26S proteasome (PDB: 5GJR), 95% were satisfied with Cα-Cα distances ≤ 30 Å (Figure 5B,C, Table S4B). Similarly, the pre-mRNA spliceosome was identified with 51 cross-links within 22 out of 44 subunits. Based on the high-resolution structure of the pre-mRNA spliceosome complex (PDB: 6QX9), 94% cross-links were satisfied within the distance threshold (≤ 30 Å) (Figure 5B,D, Table S4C). The human ribosome nascent chain complex was the best-described protein complex in our study, in which 93.6% protein composition (i.e., 73 out of 78 subunits) was identified with a total of 875 unique K-K linkages. However, when mapped onto an available high-resolution structure (PDB: 6OLG), only 76% of the 654 cross-links satisfied the 30 Å distance limit (Figure S4 and Table S4D)—noticeably lower than the overall distance satisfaction rate, as well as that of the of the 26S proteasome and pre-RNA spliceosome complexes (>90%). Interestingly, the out-of-distance ribosomal cross-links (> 30 Å) contributed to the majority (71%) of all non-satisfying cross-links in our entire data set. Moreover, other XL-MS studies of ribosomal complexes have yielded similar levels of cross-link distance satisfaction in cell lysates (72%)[12] and from affinity-purified samples (82%).[31] Together, these results suggest that ribosomal complexes are highly dynamic and are not well represented using a single static assembly.

Cellular Components and PPI Networks of HEK293 DSSO XL-MS Proteome

To understand the scope of the proteome targeted by *in vitro* DSSO cross-linking coupled with the SEC-HpHt workflow, we employed the Gene Ontology (GO) to analyze the cellular components represented by the 2066 proteins in our XL-proteome. As shown in Figure 4D, all major compartments have been mapped by DSSO-based XL-MS analysis with an overall distribution similar to that of the entire human proteome. However, while cytosolic and mitochondrial proteins were well represented in the XL-proteome, the number of cross-links identified among plasma membrane proteins was much less. These observations can be largely attributed to several keys factors such as differences in protein abundance and solubility, as well as the number of targetable lysines and their solvent accessibilities.[4] In general, the overall distribution of cellular compartments in the XL-proteome derived from SEC-HpHt was very similar to other published proteome-wide XL-MS studies.[7]

Finally, we utilized the 1848 interprotein and 6753 intraprotein K-K linkages identified in our XL-MS data set to generate an XL-PPI network map comprising 2066 nodes and 2615 edges, denoting 793 interprotein and 1822 intraprotein interactions (Figure S5). Thus, every interprotein and intraprotein PPIs were represented by an average of 2.3 and 3.7 cross-links, respectively, bolstering the confidence of the identified XL-PPIs. When compared to both BioGrid and BioPlex databases, 495 of our XL-PPIs were known and 298 were considered as novel interactions. Among the 298 novel interactions, 110 have been found in other XL-MS studies.[7,9,12] To better understand the captured interactions, we employed STRING scores to assess the likelihood of an interaction being true. The STRING scores were found for 463 out of the 793 known XL-PPIs identified here, and they were all above 0.4. It is noted that 89% of curated human PPIs in the STRING database have a STRING score below 0.4, displaying only low to medium confidence. In contrast, 88% of our *in*

vitro XL-PPIs have a STRING score ≥ 0.8 (Figure S6), suggesting high confidence. This observation is consistent with recent proteome-wide XL-MS studies, in which >70% of the *in vivo* XL-PPIs have STRING scores ≥ 0.9[7] and > 60% of the *in vitro* XL-PPIs have STRING scores ≥ 0.9.[8] Collectively, our SEC-HpHt based XL-MS workflow is effective in identifying the high confidence XL-PPIs.

CONCLUSION

In this study, the two-step SEC-HpHt fractionation method has been established to enhance the separation of cross-linked peptides to improve the depth of proteome-wide XL-MS analysis. The XL-MS workflow developed here has been successfully employed for DSSO-based *in vitro* XL-MS studies of HEK293 cell lysates, which produced the breadth of XL information comparable to the largest DSSO *in vitro* XL-MS data set of mammalian cell lysates,[12] but with significantly less amount of MS acquisition time. Our results have demonstrated that the SEC-HpHt strategy is effective and robust for comprehensive PPI profiling with improved throughput. This is advantageous as it would make XL-MS technologies better suited for systems-wide studies to advance biomedical research. In addition, this analytical strategy can be easily adopted for other cross-linker-based XL-MS analyses and can be coupled with an affinity purification-based enrichment strategy to further enlarge the scope of XL-proteomes in the future.

Supplementary Material

Refer to Web version on PubMed Central for supplementary material.

ACKNOWLEDGMENTS

The authors wish to thank Prof. A.L. Burlingame, Drs. Peter Baker and Robert Chalkley for their support of Protein Prospector. This work was supported by National Institutes of Health grants R01GM074830 and R01GM130144 to L.H.

ABRREVIATION

XL-MS	cross-linking mass spectrometry
AP-MS	affinity purification mass spectrometry
2D	two-dimensional
DSSO	disuccinimidyl sulfoxide
MS	mass spectrometry
MS^n	multi-stage tandem mass spectrometry
PPI	protein-protein interaction
HpH	high pH reverse phase
HpHt	high pH reverse phase tip

SEC	size-exclusion chromatography
SCX	strong cation exchange chromatography
HILIC	hydrophilic interaction liquid chromatography
ChaFRADIC	charge-based fractional diagonal chromatography
hSAX	hydrophilic strong anion exchange
LC MS^n	liquid chromatography multistage tandem mass spectrometry
CSM	cross-link peptide spectrum match
FDR	false discovery rate

REFERENCES:

(1). Bludau I; Aebersold R Nat. Rev. Mol. Biol 2020, 21, 327–340.

(2). Huttlin EL; Bruckner RJ; Navarrete-Perea J; Cannon JR; Baltier K; Gebreab F; Gygi MP; Thornock A; Zarraga G; Tam S Cell 2021, 184, 3022–3040. e28. [PubMed: 33961781]

(3). Leitner A; Faini M; Stengel F; Aebersold R Trends Biochem. Sci 2016, 41, 20–32. [PubMed: 26654279]

(4). Yu C; Huang L Anal. Chem 2018, 90, 144–165. [PubMed: 29160693]

(5). Sinz A Angew. Chem., Int. Ed 2018, 57, 6390–6396.

(6). Steigenberger B; Albanese P; Heck AJR; Scheltema RA J. Am. Soc. Mass Spectrom 2020, 31, 196–206. [PubMed: 32031400]

(7). Wheat A; Yu C; Wang X; Burke AM; Chemmama IE; Kaake RM; Baker P; Rychnovsky SD; Yang J; Huang L Proc. Natl. Acad. Sci. U.S.A 2021, 118, No. e2023360118. [PubMed: 34349018]

(8). Gotze M; Iacobucci C; Ihling CH; Sinz A Anal. Chem 2019, 91, 10236–10244. [PubMed: 31283178]

(9). Liu F; Lössl P; Scheltema R; Viner R; Heck AJ Nat. Commun 2017, 8, No. 15473. [PubMed: 28524877]

(10). Chavez JD; Wippel HH; Tang X; Keller A; Bruce JE Chem. Rev 2021, DOI: 10.1021/acs.chemrev.1c00223.

(11). Fasci D; van Ingen H; Scheltema RA; Heck AJ Mol. Cell. Proteomics 2018, 17, 2018–2033. [PubMed: 30021884]

(12). Yugandhar K; Wang T-Y; Leung AK-Y; Lanz MC; Motorykin I; Liang J; Shayhidin EE; Smolka MB; Zhang S; Yu H Mol. Cell. Proteomics 2020, 19, 554–568. [PubMed: 31839598]

(13). Fürsch J; Kammer K-M; Kreft SG; Beck M; Stengel F Anal. Chem 2020, 92, 4016–4022. [PubMed: 32011863]

(14). Herzog F; Kahraman A; Boehringer D; Mak R; Bracher A; Walzthoeni T; Leitner A; Beck M; Hartl FU; Ban N; Malmstrom L; Aebersold R Science 2012, 337, 1348–1352. [PubMed: 22984071]

(15). Gutierrez C; Chemmama IE; Mao H; Yu C; Echeverria I; Block SA; Rychnovsky SD; Zheng N; Sali A; Huang L Proc. Natl. Acad. Sci. U.S.A 2020, 117, 4088–4098. [PubMed: 32034103]

(16). Kaake RM; Wang X; Burke A; Yu C; Kandur W; Yang Y; Novtisky EJ; Second T; Duan J; Kao A Mol. Cell. Proteomics 2014, 13, 3533–3543. [PubMed: 25253489]

(17). Chavez JD; Lee CF; Caudal A; Keller A; Tian R; Bruce JE Cell Syst. 2018, 6, 136–141. e5. [PubMed: 29199018]

(18). Tan D; Li Q; Zhang M-J; Liu C; Ma C; Zhang P; Ding Y-H; Fan S-B; Tao L; Yang B eLife 2016, 5, No. e12509. [PubMed: 26952210]

(19). Steigenberger B; Pieters RJ; Heck AJ; Scheltema RA ACS Cent. Sci 2019, 5, 1514–1522. [PubMed: 31572778]

(20). Fritzsche R; Ihling CH; Götze M; Sinz A Rapid Commun. Mass Spectrom 2012, 26, 653–658. [PubMed: 22328219]

(21). Leitner A; Reischl R; Walzthoeni T; Herzog F; Bohn S; Forster F; Aebersold R Mol. Cell. Proteomics 2012, 11, No. M111 014126.

(22). Tinnefeld V; Venne AS; Sickmann A; Zahedi RP J. Proteome Res 2017, 16, 459–469. [PubMed: 28054782]

(23). Giese SH; Sinn LR; Wegner F; Rappsilber J Nat. Commun 2021, 12, No. 3237. [PubMed: 34050149]

(24). Wu Z; Li J; Huang L; Zhang X Anal. Chim. Acta 2021, 1179, No. 338838. [PubMed: 34535262]

(25). Lenz S; Sinn LR; O'Reilly FJ; Fischer L; Wegner F; Rappsilber J Nat. Commun 2021, 12, No. 3564. [PubMed: 34117231]

(26). Yang F; Shen Y; Camp DG 2nd; Smith RD Expert Rev. Proteomics 2012, 9, 129–134. [PubMed: 22462785]

(27). Fang F; Zhao Q; Chu H; Liu M; Zhao B; Liang Z; Zhang L; Li G; Wang L; Qin J Mol. Cell. Proteomics 2020, 19, 1724–1737. [PubMed: 32675193]

(28). Yu C; Huszagh A; Viner R; Novitsky EJ; Rychnovsky SD; Huang L Anal. Chem 2016, 88, 10301–10308. [PubMed: 27626298]

(29). Kao A; Chiu C.-l.; Vellucci D; Yang Y; Patel VR; Guan S; Randall A; Baldi P; Rychnovsky SD; Huang L Mol. Cell. Proteomics 2011, 10, No. M110.002212.

(30). Wilhelm M, et al. Nature 2014, 509, 582–587. [PubMed: 24870543]

(31). Tuting C; Iacobucci C; Ihling CH; Kastritis PL; Sinz A Sci. Rep 2020, 10, No. 12618. [PubMed: 32724211]

- Experimental details including materials and methods and describing performance evaluation of 2D SEC-HpHt separation in proteome-wide XL-MS analysis and data comparison with published results (PDF)
- Data comparison among the two published proteome-wide XL-MS studies and this work (XLSX)
- Detailed summary of unique DSSO cross-linked peptides of HEK 293 cell lysates identified by LC MS^n (XLSX)
- CORUM analysis of protein complexes in the XL-proteome (XLSX)
- Distance mapping of DSSO cross-links onto the known structures of the 111 protein complexes (XLSX)

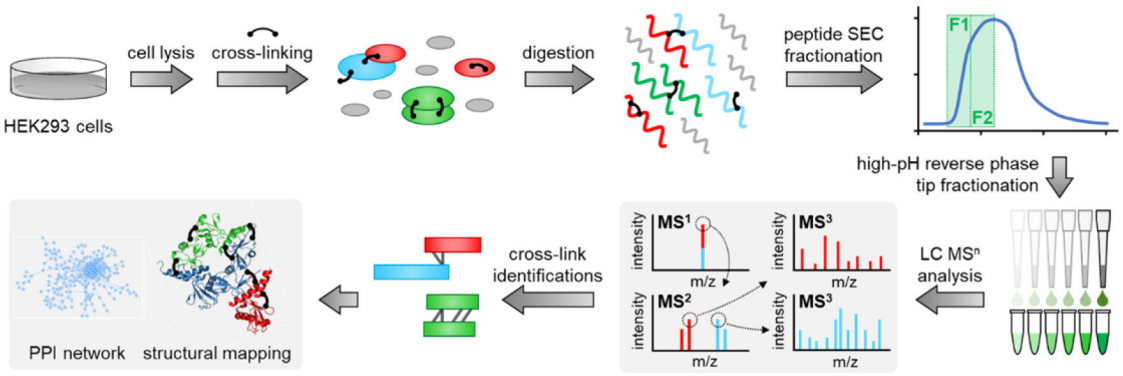

Figure 1.

General *in vitro* XL-MS workflow coupled with the 2D SEC-HpHt fractionation method.

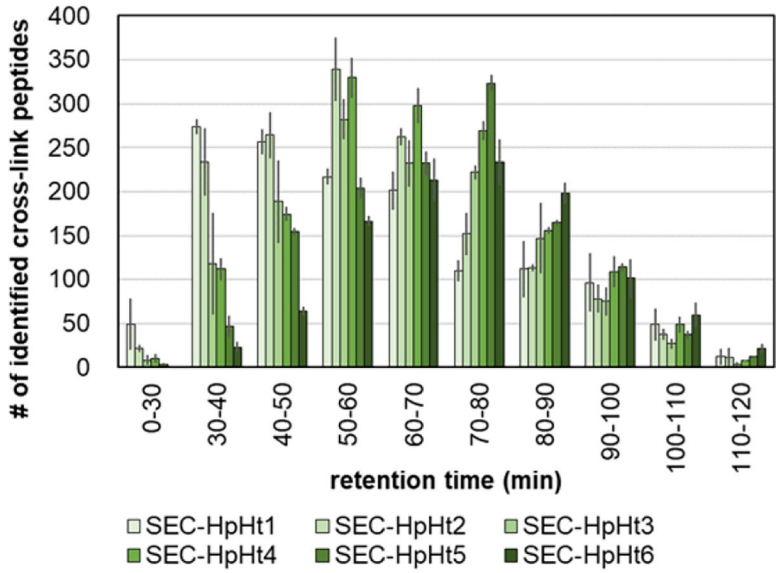

Figure 2.

Evaluation of separation orthogonality of SEC-HpHt fractions during LC MS^n analysis. The number of cross-linked peptides identified from each of the six SEC-HpHt fractions was plotted with their corresponding elution times.

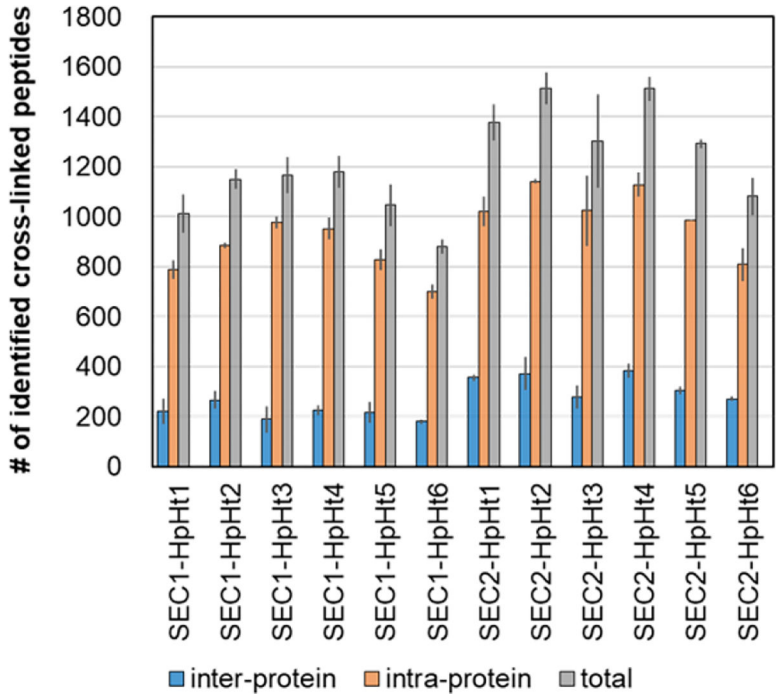

Figure 3.

Distribution of the average number of redundant cross-linked peptides identified in SEC-HpHt fractions obtained from three biological replicates. There were a total of 12 SEC-HpHt fractions (SEC1-HpHt:1-6 and SEC2-HpHt:1-6) in each XL-MS experiment.

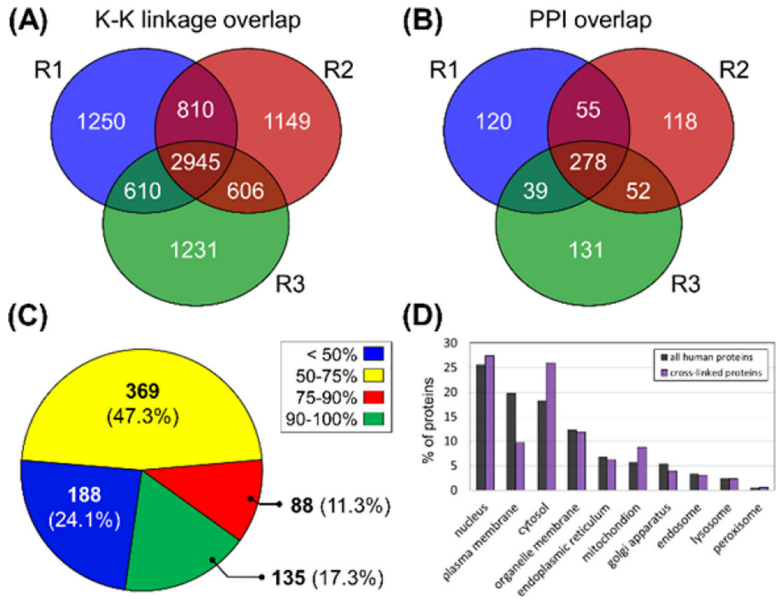

Figure 4.

Evaluation of XL-MS data reproducibility and proteome contents. Overlaps of unique (A) K-K linkages and (B) PPIs among three biological replicates. R1-R3: replicate 1–3. (C) Distribution of protein composition coverage of CORUM protein complexes identified by XL-MS analysis. (D) Gene Ontology analysis of cellular components in the XL-proteome.

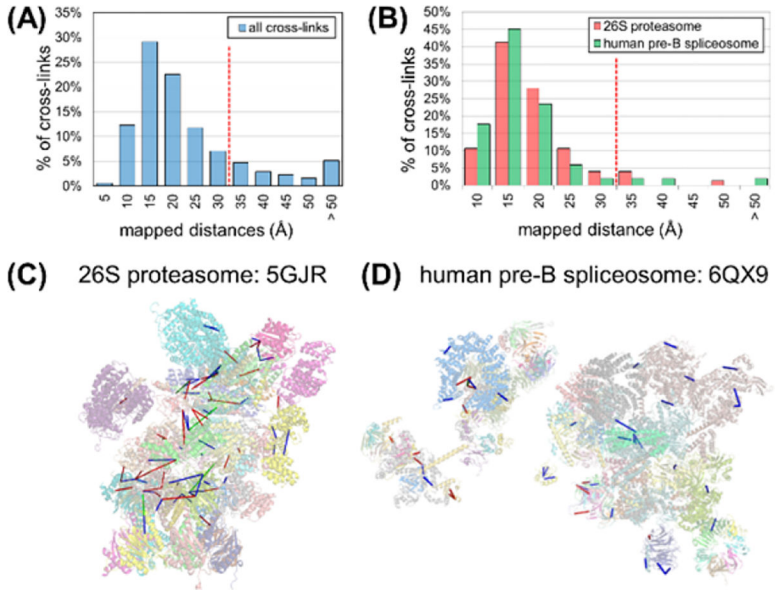

Figure 5.

Distance distribution of cross-links onto available high-resolution structures in PDB. Distance distributions of the identified cross-links onto the structures of (A) 111 protein complexes and (B) human 26S proteasome (PDB: 5GJR) and pre-B spliceosome (PDB: 6QX9) complexes, respectively. The latter was further illustrated by cross-link structural mapping in (C) 26S proteasome and (D) pre-B spliceosome complexes. Red lines: interprotein cross-links; blue lines: intraprotein cross-links; green lines: cross-links exceeding the distance threshold of 30 Å.